The Negative Phase of the Blast Load

by

Sam E. Rigby, Andrew Tyas, Terry Bennett, Sam D. Clarke, Stephen D. Fay

The Negative Phase of the Blast Load

Sam E. Rigby[a]*, Andrew Tyas[a,b],
Terry Bennett[c], Sam D. Clarke[a], Stephen D. Fay[a,b]
[a]Department of Civil & Structural Engineering, University of Sheffield,
Mappin Street, Sheffield, S1 3JD, UK.
[b]Blastech Ltd., The BioIncubator,
40 Leavygreave Road, Sheffield, S3 7RD, UK.
[c]School of Civil, Environmental & Mining Engineering,
North N136, North Terrace Campus, The University of Adelaide,
SA 5005, Australia

ABSTRACT

Following the positive phase of a blast comes a period where the pressure falls below atmospheric pressure known as the negative phase. Whilst the positive phase of the blast is well understood, validation of the negative phase is rare in the literature, and as such it is often incorrectly treated or neglected altogether. Herein, existing methods of approximating the negative phase are summarised and recommendations of which form to use are made based on experimental validation. Also, through numerical simulations, the impact of incorrectly modelling the negative phase has been shown and its implications discussed.

Key words: Blast; Dynamic response; Experiment; Negative phase; SDOF; Validation

1. INTRODUCTION

An explosion is characterised by the rapid release of energy as a mass of reactive material is converted into an extremely dense region of high pressure gas. This gas rapidly expands and displaces the surrounding air, causing a pressure disturbance – a blast wave – to propagate away from the centre of the explosive at supersonic speed. As the blast wave travels through the air, the front of the pressure disturbance 'shocks up', resulting in a near-discontinuous increase in pressure, density and temperature. Following the shock front the pressure decays until ambient pressure is reached, the duration of which is known as the positive phase duration. The positive phase of the blast load acting on a structure can be described by the semi-empirical 'modified Friedlander equation' [1]

$$p_r(t) = p_{r,\max}\left(1 - \frac{t}{t_d}\right)e^{-bt/td} \qquad (1)$$

---

*Corresponding author. Tel.: + 44 (0) 114 222 5724. *Email address*: sam.rigby@sheffield.ac.uk

where $p_{r,\max}$ is the peak reflected pressure, t_d is the positive phase duration and b is the coefficient that describes the rate of decay of the pressure-time curve, known as the waveform or decay parameter.

Following the positive phase comes a period of 'negative' pressure (below atmospheric); a partial vacuum caused by over-expansion of the shocked air. An idealised pressure-time profile for a reflected blast wave is shown in Figure 1, where $p_{r,min}$ is the peak underpressure, t_d^- is the negative phase duration, and the positive and negative phase impulses, i_r and i_r^-, are given as the temporal integral of the positive phase pressure and negative phase pressure respectively.

1.1. LITERATURE REVIEW

The influence of the negative phase has become a topic of increased interest over recent years, in particular the effect of the negative phase on light cladding and glazing panels. This perhaps reflects the growing awareness of the importance of well-designed glazing in minimising damage to infrastructure and injuries to building inhabitants in the event of an explosion. Indeed, it has been suggested that the majority of non-fatal injuries from terrorist attacks are caused by either airborne glass fragments or damage to hearing from failed glass panels [2].

Krauthammer and Altenberg [3] studied the influence of the negative phase on the failure of laminated glass panels using a simplified numerical model. The research showed that it is possible for the panel to be undamaged by the positive phase of the blast load, yet a combination of negative phase pressure and elastic rebound may cause failure of the glass panel *towards* the source of the blast. Wei & Dharani [4, 5] and Larcher et al. [6] also studied laminated glass panels, and highlighted instances where the midspan displacement and stresses within the panel can be as much as twice those caused by the positive phase.

Teich and Gebbeken [7] took a more general approach by conducting a parametric study on elastic single-degree-of-freedom (SDOF) systems to quantify the effect of the negative phase relative to the effect of the positive phase alone. It was found that for certain configurations of scaled distance and dynamic target properties, inclusion of the negative phase in the model could cause midspan displacement of up to an order of magnitude greater than that of the positive phase. This study has been extended to quantify the effect on cable net facades [8, 9]. Bryant et al. [10] provided both numerical and experimental examples of situations where the
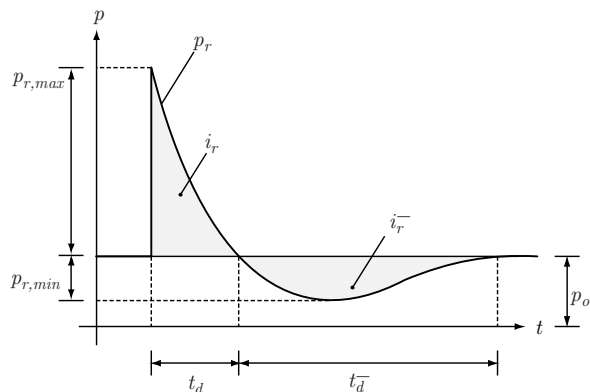

Figure 1. Idealised pressure-time profile for a reflected blast wave

negative phase causes adverse target response, and also highlighted the limitations of shock tube testing to accurately replicate free-field negative phase pressures and impulses, on account of the inability of a shock tube to replicate the effect of the rising fireball [11].

Whilst these studies show that the negative phase cannot be ignored for certain blast scenarios, and indeed some effort has been undertaken to define the situations where ignoring the negative phase is un-conservative, there remains some uncertainty on the issue of how to properly model the form of the negative phase pressure-time history. The purpose of the paper is therefore two-fold. Firstly, existing methods of modelling the negative phase will be summarised and recommendations of which form to use will be made based on experimental validation. Secondly, through numerical simulations, the impact of ignoring or incorrectly modelling the negative phase will be shown and its implications discussed.

2. PREDICTING BLAST WAVE PARAMETERS

The positive phase of the blast load is well understood, with the Kingery and Bulmash [12] empirical blast parameters well-established in the current literature [13, 14, 15]. These blast predictions are implemented into the automated predictive tool ConWep [16]. Bogosian et al. [17] showed that there was generally good correlation between the Kingery and Bulmash (KB) predictions and empirical data from blast trials, but with some considerable spread. It is possible that this was due to the fact that the empirical data was generally from field trials involving very large explosions, with the consequent difficulties in carefully controlling the test parameters. Recent work by the authors [18, 19] indicates that in small scale, carefully controlled experimental trials, the correlation between empirical data and the KB predictions for the positive phase parameters is remarkably good.

Negative phase parameters are also available in the literature [13, 15]. However, as Bogosian et al. [17] noted in their review, *"The precise provenance of these curves is unknown at the present time."* They suggested that this uncertainty is due in part to the fact that *"Not all (experimental data records) were of sufficient duration and/or quality as to be able to extract negative as well as positive values, and while some had dubious peak pressure readings, others became suspect at later time and therefore could not produce reliable impulses."* This is perhaps inevitable in the large scale experimental tests that formed the basis of the data analysed in that work.

The original source of the negative phase parameters presented in [13] is unclear, although a thorough review of the available literature as part of the current study indicates that it may have been from analytical work conducted in the 1950 s by Granström [20]. Figure 2 shows the relationship between reflected positive and negative phase blast parameters with scaled distance,

$$Z = \frac{R}{\sqrt[3]{W}} \qquad (2)$$

where R is the distance from the target to the source of the explosive and W is the mass of explosive expressed as an equivalent mass of TNT. Note that impulse and time parameters are scaled by the cube root of the charge mass, after Hopkinson-Cranz scaling [21].

In this study, simplified parameter expressions have been determined by digitizing the negative phase data presented in [13] and fitting curves to the data points. Relationships for negative reflected pressure and impulse (for hemispherical surface bursts) are given in equations 3 and 4 respectively, and can be used to determine the relevant loading parameters.
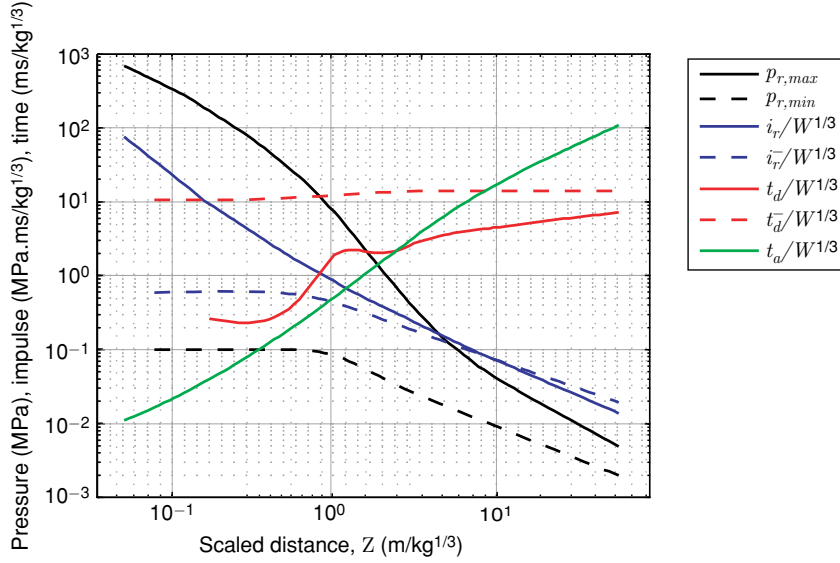
Figure 2. Positive and negative phase reflected blast wave parameters for hemispherical charges of TNT on the surface (12, 13)

$$p_{r,\min}(Z) = \begin{cases} 101, & 0.071 < Z \le 0.668 \\ -32.9Z^2 + 13.0Z + 106, & 0.668 < Z \le 1.27 \\ 93.0Z^{-1.22}, & 1.27 < Z \le 2.78 \\ 73.0Z^{-0.978}, & 2.78 < Z \le 37.6 \end{cases} \quad \text{(kPa)} \qquad (3)$$

$$i_r^-(Z) = \sqrt[3]{W} \times \begin{cases} -724Z^2 + 445Z + 553, & 0.071 < Z \le 0.580 \\ 11.4Z^2 - 315Z + 752, & 0.580 < Z \le 1.19 \\ 462Z^{-0.880}, & 1.19 < Z \le 5.25 \\ 434Z^{-0.842}, & 5.25 < Z \le 37.6 \end{cases} \quad \text{(kPa.ms)} \quad (4)$$

For small scaled distances, the peak underpressure and negative phase impulse are very small relative to the positive phase. It is clear, however, from Figure 2 that this observation is only true for small values of Z, and that the negative phase impulse approaches that of the positive phase for larger scaled distances and eventually exceeds the positive phase impulse when $Z > 8$. In free-field blast experiments, the rising fireball creates a lower pressure near the ground surface, which draws in the surrounding air. This has the effect of further lowering the air density, which has already been over-expanded after the shockwave has passed, and hence results in larger negative phase impulses at larger stand-off distances [11].

3. THE FORM OF THE NEGATIVE PHASE

3.1. LINEAR APPROXIMATION

One way of modelling the blast pressure is with a piecewise linear function, as is the approach of Krauthammer and Altenberg [3]. The positive phase is approximated as a linearly decaying triangular pulse, with the linear load duration, $t_{d,lin}$, set such that the impulse given by the triangular load matches that given by the empirical method, i.e. $t_{d,lin} = 2i_r/p_{r,\max}$. The negative phase is modelled as a bilinear approximation with a rise time equal to 1/4 of the negative phase duration. As per the positive phase, the linear negative phase duration, $t_{d,lin}^-$, is specified to preserve negative phase impulse, i.e. $t_{d,lin}^- = 2i_r^-/p_{r,\min}$. The negative phase begins at t_d, rather than $t_{d,lin}$, giving a period of zero pressure between the linear positive and negative phase. This approach is also recommended in UFC-3-340-02 [13], with the piecewise expression given in equation 5.

$$
p_r(t) = \begin{cases}
p_{r,\max}\left(1 - \dfrac{t}{t_{d,lin}}\right), & t \leq t_{d,lin} \\
0, & t_{d,lin} < t \leq t_d \\
-p_{r,\min}\left(\dfrac{t - t_d}{0.25 t_{d,lin}^-}\right), & t_d < t \leq t_d + 0.25 t_{d,lin}^- \\
-p_{r,\min}\left(1 - \dfrac{t - (t_d + 0.25 t_{d,lin}^-)}{0.75 t_{d,lin}^-}\right), & t_d + 0.25 t_{d,lin}^- < t \leq t_d + t_{d,lin}^-
\end{cases}
\tag{5}
$$

3.2. EXTENDED FRIEDLANDER

Another common method of modelling the negative phase is to simply extend the Friedlander equation (1) to $t = \infty$, rather than truncating the expression at t_d. This is the approach adopted by Wei & Dharani [4, 5], Gantes [22] and the *LOAD_BLAST subroutine in LS-DYNA [23]. Given the ConWep positive phase parameters for pressure, duration and impulse, the waveform parameter can be determined by integrating the Friedlander expression over the positive phase to give

$$
i_r = \int_0^{t_d} p_{r,\max}\left(1 - \frac{t}{t_d}\right) e^{-bt/t_d} = \frac{p_{r,\max} t_d}{b^2}\left(b - 1 + e^{-b}\right)
\tag{6}
$$

which can be solved iteratively to determine the value of b which gives the correct impulse at that particular scaled distance.

As the negative phase is also constructed from this expression, it is clear that the form of this negative phase is entirely dependent on the positive phase parameters. As such there are no variables to control negative phase pressure and impulse – the values given by this approximation may not match the empirical predictions. Integrating the negative phase of the Friedlander equation gives the impulse as

$$i_r^- = \int_{t_d}^{\infty} p_{r,\max}\left(1 - \frac{t}{t_d}\right)e^{-bt/t_d} = \frac{p_{r,\max}t_d}{b^2}e^{-b}, \tag{7}$$

at $Z = 10$ m/kg$^{1/3}$, for example, ConWep gives $p_{r,\max} = 31.54$ kPa, $i_r/W^{1/3} = 59.33$ kPa.ms/kg$^{1/3}$ and $t_d/W^{1/3} = 4.788$ ms/kg$^{1/3}$. Iterating equation 6 gives the waveform parameter, $b = 0.771$. When these parameters are used as input in equation 7, the negative phase impulse is given as $i_r^-/W^{1/3} = 118$ kPa.ms/kg$^{1/3}$, whereas the parameter relationship in the literature, shown in Figure 2 and equation 4, gives the negative phase impulse as $i_r^-/W^{1/3} = 62$ kPa.ms/kg$^{1/3}$.

3.3. EXTENDED FRIEDLANDER WITH TEICH C_r^-

In order to better control the form of the negative phase, Teich & Gebbeken [7] introduce the negative phase reflection coefficient, C_r^-, which is a function of the scaled distance,

$$C_r^- = \frac{1.9Z - 0.45}{Z} \text{ for } Z > 05 \tag{8}$$

and also offer a scaled distance relationship for an improved waveform parameter

$$\alpha = 1.5Z^{-0.38} \text{ for } 0.1 < Z < 30. \tag{9}$$

This enables the value of extended Friedlander peak underpressure to be better matched to the published empirical value at that particular scaled distance (e.g. Figure 2 and equation 3), giving the piecewise positive and negative phase expression[1] as

$$p_r(t) = \begin{cases} p_{r,\max}\left(1 - \dfrac{t}{t_d}\right)e^{-\alpha\frac{t}{t_d}}, & t \leq t_d \\[3mm] C_r^- p_{so,\max}\left(1 - \dfrac{t}{t_d}\right)e^{-\alpha\frac{t}{t_d}}, & t \leq t_d \end{cases} \tag{10}$$

Although the introduction of the negative phase reflection coefficient allows the peak negative phase pressure to be controlled, the new waveform parameter, α, is again given to match the *positive phase* impulse of the Friedlander expression to empirical predictions, i.e. there remains no variable to control the negative phase impulse.

The Teich extended Friedlander gives the negative phase impulse as

$$i_r^- = \int_{t_d}^{\infty} C_r^- p_{so,\max}\left(1 - \frac{t}{t_d}\right)e^{-\alpha t/t_d} = \frac{C_r^- p_{so,\max}t_d}{\alpha^2}e^{-\alpha}, \tag{11}$$

where, for $Z = 10$ m/kg$^{1/3}$, the ConWep peak incident pressure, $p_{so,\max} = 14.81$ kPa and the reflection coefficient and waveform parameter, $C_r^- = 1.855$ and $\alpha = 0.625$ from

---

[1]In Teich and Gebbeken's formulation, $p_{r,max}$ is replaced by $C_r p_{so,max}$, however for consistency with the positive phase expressions in this article, the former notation is adopted

equations 8 and 9 respectively, gives the Teich extended Friedlander negative phase impulse as $i_r^-/W^{1/3} = 180$ kPa.ms/kg$^{1/3}$. Again this is far greater than the empirical prediction. Furthermore, in both 'extended Friedlander' approaches, the blast pressure will have a finite pressure value (albeit very small) for *all* values of t, hence the duration of the load, and also the impulse, cannot always be accurately captured with an extended Friedlander expression.

3.4. CUBIC NEGATIVE PHASE

Alternatively, the blast load can be constructed as a piecewise pressure-time function using the Friedlander positive phase [21] and a cubic expression for the negative phase, shown in equation 12. This negative phase expression is given by Granström [20], and, although the origin of the expression is unclear, it appears as though it is a fit to early numerical simulations. It is worth noting that the negative phase expression given does not vary with scaled distance and instead is a general fit to the *form* of the negative phase. The Granström expression is recommended by the Naval Facilities Engineering Command Design Manual 2.08, *Blast Resistant Structures* [24], and the US Army Blast Effects Design Spreadsheet (SBEDS) [25].

$$p_r(t) = \begin{cases} p_{r,\max}\left(1 - \dfrac{t}{t_d}\right)e^{-b\frac{t}{t_d}}, & t \leq t_d \\[4mm] -p_{r,\min}\left(\dfrac{6.75(t-t_d)}{t_d^-}\right)\left(1 - \dfrac{(t-t_d)}{t_d^-}\right)^2, & t_d < t \leq t_d + t_d^- \end{cases} \tag{12}$$

With this expression, the negative phase duration is corrected such that the integral of the cubic expression gives the same impulse as that given by the empirical prediction in equation 4, i.e. $t_d^- = 16i_r^-/9p_{r,\min}$.

Figure 3 shows normalised pressure-time histories for the different negative phase approximations at $Z = 4$ and $Z = 16$ m/kg$^{1/3}$. It is clear that the choice of negative phase approximation has a significant impact on the form of the blast pressure history.

4. EXPERIMENTAL VALIDATION OF NEGATIVE PHASE APPROXIMATIONS

The lack of agreement between the different negative phase expressions highlights the need for a well validated negative phase model. In this section, a simple experimental validation is provided and recommendations are given on which approximation to use.

A number of blast trials were conducted at the University of Sheffield Blast & Impact Laboratory, Buxton, UK. 0.25 kg PE4 hemispherical explosive charges were detonated 4 m, 6 m, 8 m and 10 m away from and orthogonal to the external wall of a reinforced concrete bunker, forming a large, effectively rigid target, such that fluid-structure interaction effects [26, 27] could be ignored. The charges were detonated on a 50 mm thick steel plate, placed on a level, flat concrete ground slab, enabling the detonation to be considered as a hemispherical surface burst. A Kulite HKM 7 bar pressure gauge was placed 375 mm from the base of the target, and pressure was recorded using a 16-Bit Digital Oscilloscope at a sample rate of 100 kHz, synchronised with the detonation.
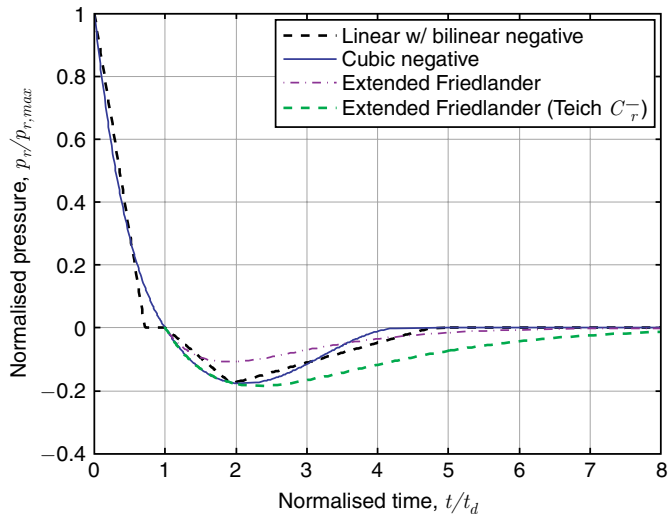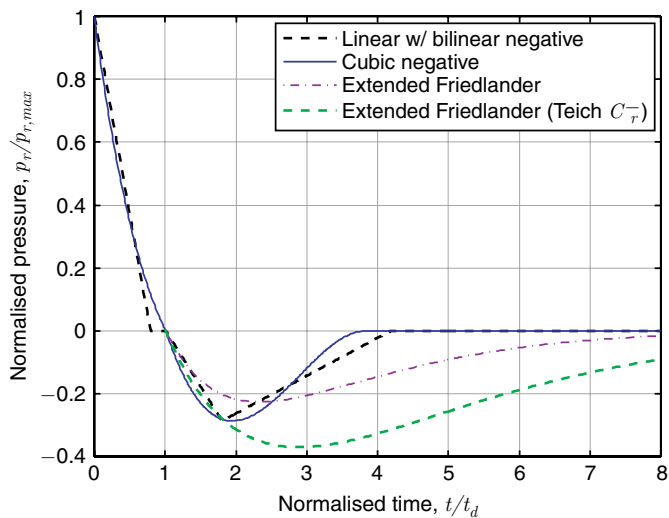
(a) $Z = 4$

(b) $Z = 16$

Figure 3. Normalised positive and negative phase approximations for $Z = 4$ and $Z = 16$ m/kg$^{1/3}$

4.1. EXPERIMENTAL FEATURES

Figure 4 shows, as an example, the experimental trace from the 6 m shot, where the clear presence of the well-known 'second shock' [28] can be seen. This phenomenon is not accounted for in any of the empirical predictions, and its influence has been discounted in this study – its influence will be second order compared to the negative phase. In the test arrangement, the minimum distance from the pressure gauge to the top edge of the bunker wall was 4 m – a clearing wave travelling at 340 m/s from the nearest free edge would take ~11.5 ms to reach the gauge location before it could begin to affect the pressure readings.
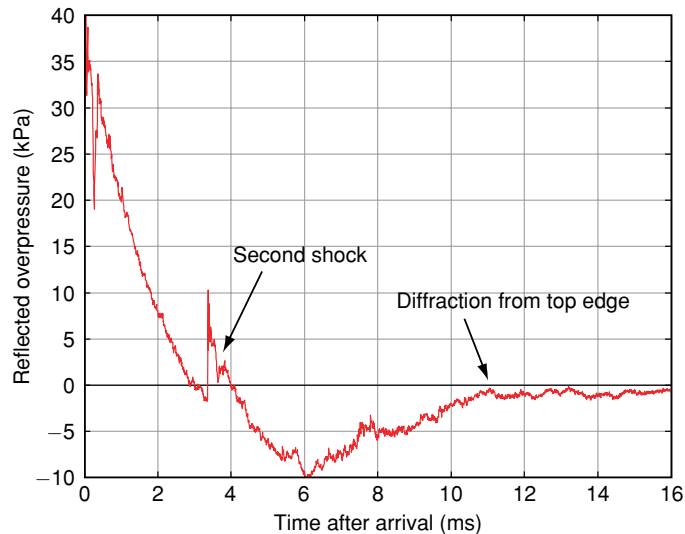
Figure 4. Experimental trace for 0.3 kg TNT at 6 m, with second shock and diffraction features annotated

Again, this can be seen in the experimental readings in Figure 4 and perhaps more clearly in Figure 5. This feature should be noted in subsequent analysis, but is clearly of relatively low relevance and the trace can be considered to be almost unaffected by clearing. The distance from the pressure gauge to the side edges of the bunker wall was greater than 4 m, ensuring that clearing effects from the side edges could be neglected.

4.2. VALIDATION

Figure 5 shows the experimental and predicted negative phase pressure-time histories and Figure 6 shows the experimental and predicted impulse-time histories. Negative phase approximations were constructed assuming a 1.20 TNT equivalence of PE4 [18], giving a charge mass, W, of 0.3 kg and scaled distances of 6.0, 9.0, 12.0 and 14.9 m/kg$^{1/3}$.

Apart from the second shock at the beginning of the negative phase (annotated in Figure 4) on the experimental traces, the cubic negative phase matches the experimental traces remarkably well, both in terms of peak negative pressure and general form of the negative phase. The linear expression gives a good approximation to the peak underpressure but is not quite as accurate at matching the shape of the negative phase. Neither extended Friedlander expressions match the experimental traces very well, particularly for the larger scaled distances.

Table 1 gives the values of peak impulse determined from the experimental traces and the negative phase approximations shown in Figure 6 – the time axis is truncated at 25 ms after detonation, before the extended Friedlander expressions reach their peak impulse value, which can be determined from the equations given in the previous section. The cubic expression can model the negative phase impulse to within 10–25% of the experimental values – the over-prediction can be primarily attributed to neglecting the second shock. The linear negative phase expression and cubic expressions are impulse-corrected to match the values given by the empirical parameter relationships; hence their impulse values are the same despite the waveforms being different. It is worth pointing out that the positive phase
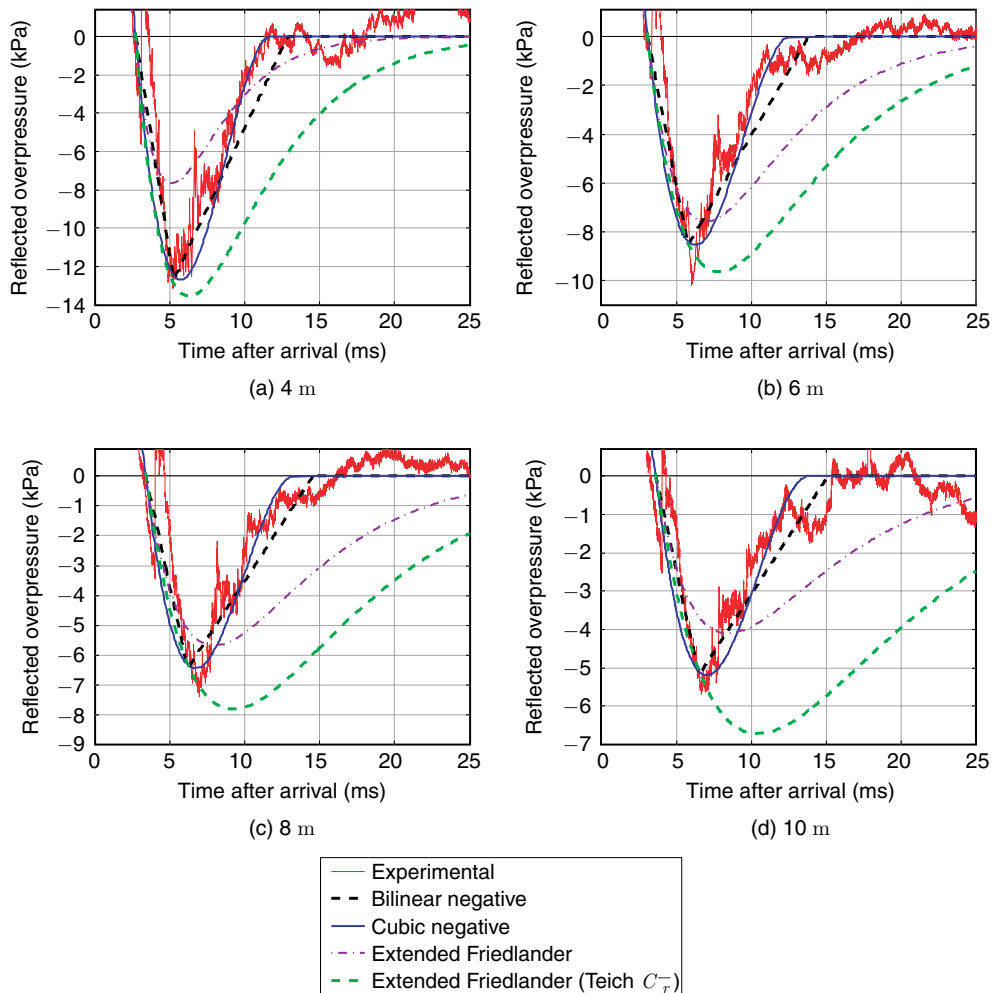
Figure 5. Negative phase approximations for a 0.25 kg hemispherical PE4 (0.3 kg TNT) charge

impulse predictions from ConWep matched the experimental positive phase impulse to within 5% for the whole test series.

To further illustrate the difference in impulses given by the negative phase approximations, Figure 7 shows the relationship between normalised net impulse ($[i_r + i_r^-]/i_r$) and scaled distance, Z. Here it can be seen how much the extended Friedlander approaches differ from the experimental (and cubic) impulses – the extended Friedlander expression using the Teich reflection coefficient gives a negative phase impulse of over an order of magnitude greater than the positive phase impulse for $Z > 30$ m/kg$^{1/3}$.

It is acknowledged that the negative phase requires more stringent validation as well as a larger experimental database than those provided as part of this study. However, at this stage it is clear that the empirical predictions appear to be a good indication of the loading
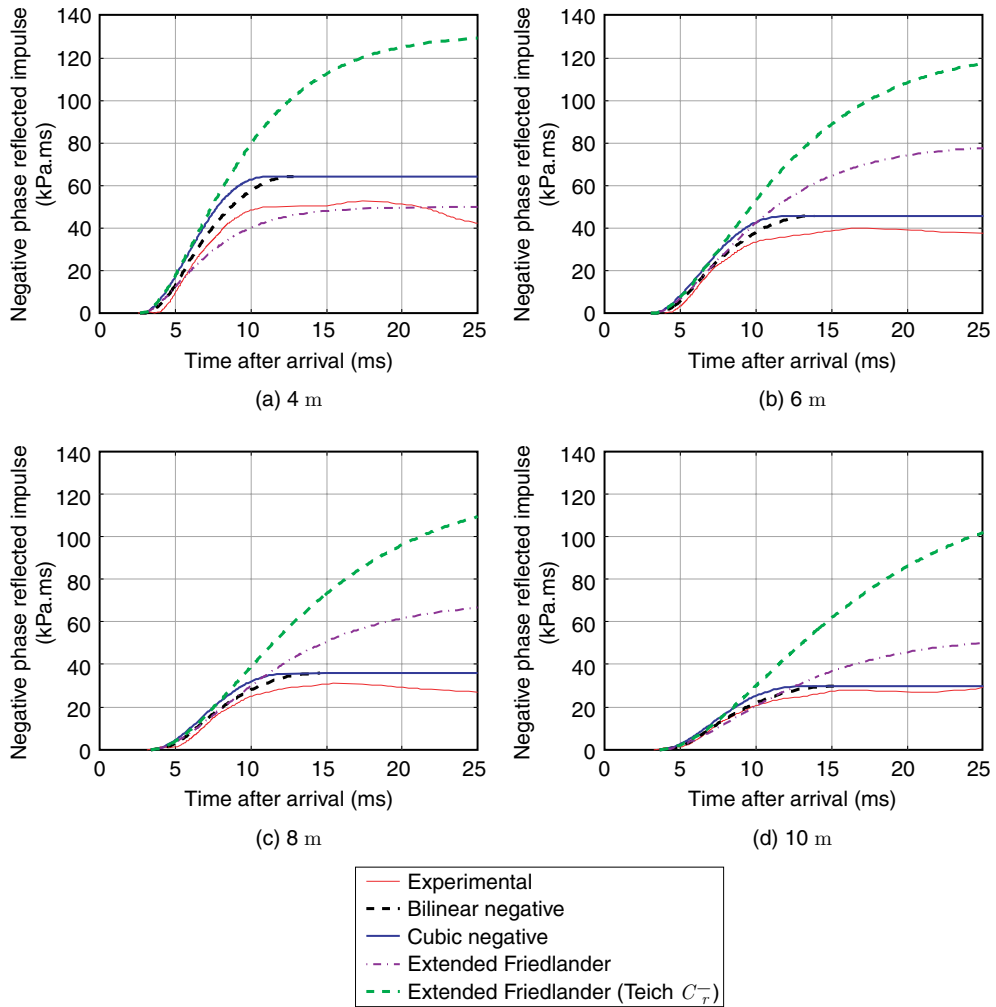
Figure 6. Negative phase impulse for a 0.25 kg hemispherical PE4 (0.3 kg TNT) charge

Table 1. Experimental and predicted negative phase reflected impulse

Load approximation	Negative phase impulse (kPa.ms)			
	Stand-off (m)			
	4	6	8	10
Experimental	52.8	39.9	31.1	27.7
Linear positive and negative	64.5	45.8	36.0	29.8
Cubic negative	64.5	45.8	36.0	29.8
Extended Friedlander	50.0	79.4	70.1	53.6
Extended Friedlander (Teich C_r^-)	126.9	119.3	118.5	120.7

Figure 7. Normalised net impulse $((i_r + i_r^-)/i_r)$ with scaled distance for different negative phase approximations

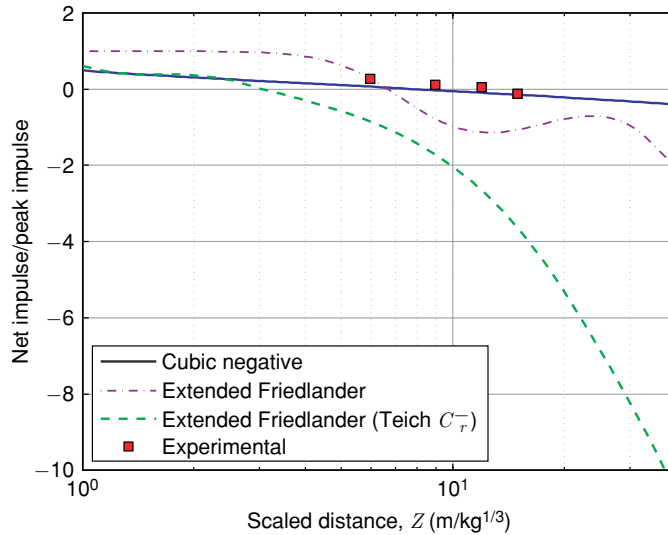parameters (for both negative and positive phases), and that the cubic negative phase not only allows better control of the negative phase to match these parameters, but also appears to follow the general form of the negative phase well.

5. MODELLING IMPLICATIONS

The first part of this paper has focussed on presenting different methods of approximating the negative phase and offered experimental validation. It is also important to demonstrate the influence that incorrectly modelling the negative phase has for certain configurations of target properties and blast event. This will be the focus of the remainder of this paper.

5.1. THE INFUENCE OF THE NEGATIVE PHASE ON ELASTIC SYSTEMS

For flexible systems subjected to blast loads, the response of the target can be modelled using the equivalent single-degree-of-freedom (SDOF) method [29]. It is common to ignore damping in blast-resistant design as it is typically only the first few cycles of displacement that are of interest, where damping has little effect [3]. In doing so, the equation of motion for an equivalent SDOF system is given as

$$m_e \ddot{z}(t) + k_e z(t) = F_e(t). \tag{13}$$

where m_e and k_e are the equivalent mass and stiffness of the system, $\ddot{z}$ and z are the acceleration and displacement of the system, and $F_e(t)$ is the equivalent externally applied load. For more information on how to transform a 'real life' system into its SDOF equivalent, the reader is referred to Biggs [29] and Morison [30].

In order to demonstrate the influence that the form of the negative phase has on elastic systems, the SDOF equivalent equation of motion was solved under the following five load cases:

- The experimental load for $R = 10$ m and $W = 0.3$ kg TNT
- A linearly decaying positive phase with *no* negative phase. This triangular pulse shape is recommended for use with the SDOF method as a 'first guess' of the typical target response to a blast load
- Friedlander positive phase with cubic negative phase (equation 12)
- Friedlander positive phase with extended Friedlander negative phase (equation 1 extended to $t = \infty$)
- Friedlander positive phase with extended Friedlander negative phase using the Teich [7] reflection coefficient (equation 10).

The linear negative phase was not modelled in this analysis. The linear expression will have the same peak negative phase pressure and impulse as the cubic expression for any scaled distance, and will therefore have little difference on target response for impulse-driven analyses. For dynamic and quasi-static analyses, however, the pulse shape has been shown to have an influence on the response of structures to blast loads [22, 31, 32], and it is therefore recommended that the cubic expression should be used in analysis, on account of it better matching the experimental pressure waveform seen in Figure 5. For the purpose of this article, however, it is more important to highlight the difference between the cubic expression, extended Friedlander expressions and neglecting the negative phase altogether, rather than focussing on the importance of pulse shape, and therefore the linear simplification of the negative phase as a bilinear pulse is not considered further.

The time ratio, t_d/T, where T is the fundamental natural period of the system, gives an indication of the response time of the structure with respect to the duration of the loading. Separate equivalent systems were analysed with time ratios of 1.00, 0.10 and 0.01 – these time ratios indicate structures whose response time is in the static, dynamic and impulsive regimes respectively. Figures 8, 9 and 10 show the normalised displacement-time histories of the equivalent SDOF systems.

From Figure 8, it is clear that the negative phase has very little effect on the peak response of flexible systems near the static regime. The system reaches peak displacement at $\sim 0.5t_d$, before the negative phase starts, hence there is little appreciable difference in the response
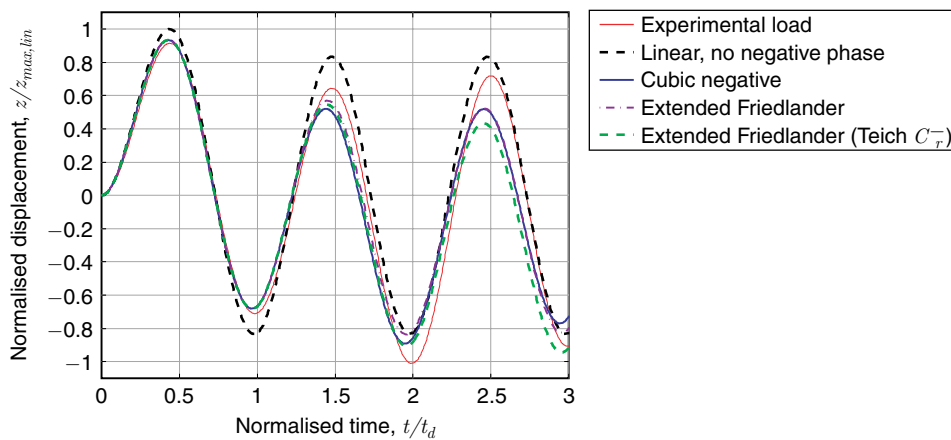

Figure 8. SDOF displacement-time histories under different negative phase approximations and experimental load for $t_d/T = 1.00$ $Z = 14.9$ m/kg$^{1/3}$ (0.3 kg TNT at 10 m)

Figure 9. SDOF displacement-time histories under different negative phase approximations and experimental load for t_d/T = 0.10 Z = 14.9 m/kg$^{1/3}$ (0.3 kg TNT at 10 m)
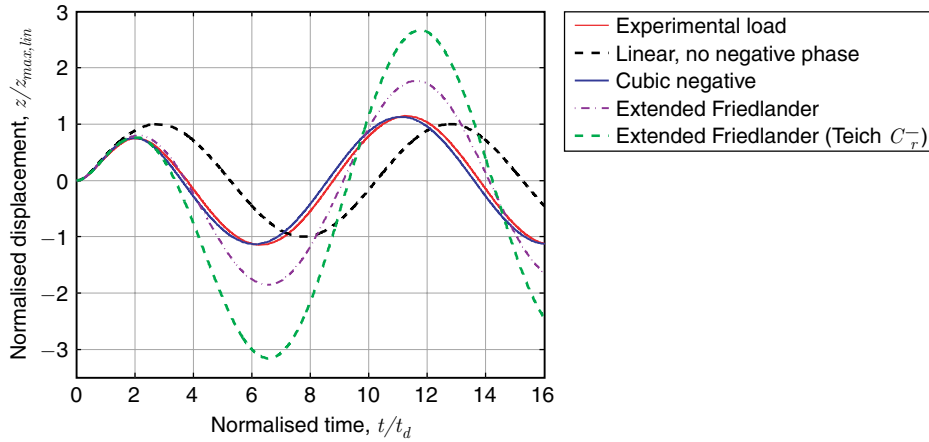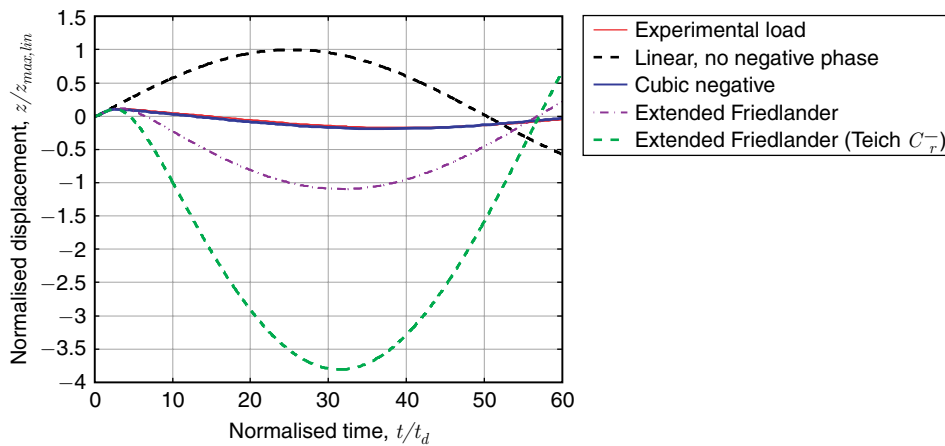

Figure 10. SDOF displacement-time histories under different negative phase approximations and experimental load for t_d/T = 0.01 Z = 14.9 m/kg$^{1/3}$ (0.3 kg TNT at 10 m)

for the different load cases – the difference in first peak response is caused only by the difference in pulse shape between the linear and exponential positive phases and not the negative phase itself.

For more flexible systems, the negative phase has a more pronounced effect, and it is for systems such as these where modelling the negative phase becomes crucial. For t_d/T = 0.1 (Figure 9), the system begins to rebound shortly after the positive phase. If the negative phase is modelled using the cubic expression, the peak rebound displacement is similar to the peak inward displacement of the system under the linear load. If the negative phase is modelled as an extended Friedlander, the rebound effect is much more pronounced. For

$t_d/T = 0.01$ (Figure 10), the system responds relatively slowly compared to the application of the load. Again, modelling the negative phase as the cubic expression gives excellent results when compared to the SDOF system under the experimental load. If the system were analysed using only the linear positive phase, the peak displacement would be over-predicted in the inward direction. If the system were analysed using the extended Friedlander approaches, the outward displacement would be grossly over-predicted, particularly if the Teich reflection coefficient is used.

The displacement ratio is given as the peak displacement of the SDOF system divided by the peak displacement of the SDOF system under the linear load [7], i.e. $z_{max}/z_{max,lin}$, and is a quantitative indicator of the influence of the negative phase on dynamic response. Values of displacement ratio for the systems analysed are summarised in Table 2.

Figure 11 shows the relationship between displacement ratio and time ratio for $Z = 14.9$ m/kg$^{1/3}$, i.e. the response spectra for elastic SDOF systems under the experimental, cubic negative and extended Friedlander load cases. For the whole range of time ratios, modelling the negative phase using the cubic approximation gives values of peak displacement that are in excellent agreement compared to the peak displacements of the SDOF system under the

Table 2. Peak normalised SDOF displacements

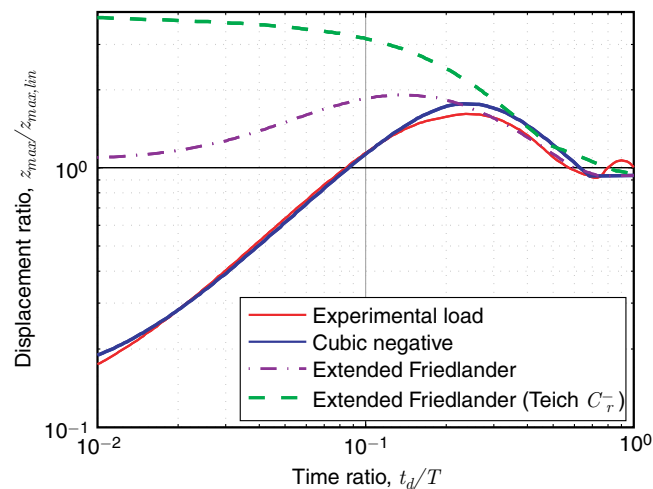| Load approximation	Displacement ratio, $z_{max}/z_{max, lin}$		
	Time ratio, t_d/T		
	1.00	0.10	0.01
Experimental	1.01	1.14	0.17
Cubic negative	0.93	1.13	0.19
Extended Friedlander	0.93	1.85	1.10
Extended Friedlander (Teich C_r^-)	0.93	3.16	3.81

Figure 11. Elastic SDOF response spectra under different negative phase approximations and experimental load for Z = 14.9 m/kg$^{1/3}$ (0.3 kg TNT at 10 m)

experimental load. The cubic negative phase accurately models the increase in peak displacement at $t_d/T \sim 0.25$ as a result of elastic rebound coinciding with negative phase pressures, as well as being able to capture the beneficial aspects of including the negative phase for impulsive loading. Modelling using either of the extended Friedlander expressions does not give acceptable results, particularly at the impulsive end of the spectrum.

Referring back to Figure 7, it is clear that the peak normalised elastic displacement of the SDOF system for impulsive loads ($t_d/T < 0.01$) is directly proportional to the normalised net impulse. At $Z = 14.9$ m/kg$^{1/3}$, the normalised net impulses for the cubic, extended Friedlander and Teich extended Friedlander are -0.2, -1.0 and -4.0 respectively, which are exactly the normalised peak displacements at the impulsive end of the response spectra. The difference in net impulse increases further when $Z > 14.9$ m/kg$^{1/3}$, which leads to the conclusion that it is vital to model the negative phase correctly at larger scaled distances.

5.2. THE INFUENCE OF THE NEGATIVE PHASE ON SYSTEMS WITH MATERIAL FAILURE

To further highlight the impact of the negative phase loading assumptions, a series of numerical analyses were performed using the explicit FE code LS-DYNA [33]. Simply supported, one-way spanning, 1 m square, 8 mm thick panels were discretised into a grid of 100×100 Belytschko-Tsay shell elements with four integration points through the thickness of the shell.

The plates were modelled as elastic-perfectly plastic using the *MAT_PLASTIC _KINEMATIC material model with Young's modulus, $E = 70$ GPa, density $\rho = 2500$ kg/m^3, Poisson's ratio, $\nu = 0.25$ and zero tangent modulus. A yield strength of 70 MPa was selected for the panels, which is within the range of values for structural glass given in [5]. The material properties are summarised in Table 3, and were selected to be indicative of a typical glazing panel.

Pressure loading was applied at nodal points as force-time histories – the models were analysed under the loading from an 8 kg hemispherical TNT surface burst at 20 m stand-off, with separate models run for the following load cases; linear positive with no negative, Friedlander positive with cubic negative, extended Friedlander and extended Friedlander with Teich reflection coefficient.

Failure strain was specified as multiples of the elastic strain limit ($\epsilon_e = \sigma_y/E$), set at 2, 4, 10 and $20\epsilon_e$ to represent increasing levels of ductile failure. If any of the elements within the plate failed, the analysis was terminated and the direction in which the panel failed was recorded.

With large displacements, fluid-structure interaction (FSI) may serve to dampen the blast

Table 3. Material properties of the plates analysed

Parameter	Symbol	Value (unit)
Young's modulus	E	70 (GPa)
Density	ρ	2500 (kg/m^3)
Poisson's ratio	ν	0.25 ($-$)
Span	L	1 (m)
Thickness	d	8 (mm)
Yield strength	σ_y	70 (MPa)
Elastic strain limit	ϵ_e	0.01 ($-$)
Failure strain	ϵ_f	2–20ϵ_e ($-$)

Table 4. Material failure for a 1 m × 1 m panel subjected to an 8 kg hemispherical TNT burst at 20 m ($Z = 10.0$ m/kg$^{1/3}$) under different negative phase approximations. '–' indicates no material failure whereas 'F_i' and 'F_o' indicate material failure in the inward and outward direction respectively

Load approximation	Panel failure			
	$\epsilon_f =$			
	$2\epsilon_e$	$4\epsilon_e$	$10\epsilon_e$	$20\epsilon_e$
Linear, no negative phase	F_i	F_i	–	–
Cubic negative	F_i	F_o	F_o	–
Extended Friedlander	F_i	F_o	F_o	F_o
Extended Friedlander (Teich C_r^-)	F_i	F_o	F_o	F_o

pressure and result in lower values of displacement. Subramaniam et al. [34] used the ratio of the peak particle velocity to peak plate velocity to quantify the influence of FSI. In this numerical study, a peak particle velocity of 88.5 m/s (from ConWep) compared to a maximum plate velocity of ∼6 m/s gives a ratio of 0.07, at which the influence of FSI is still second order. Therefore the use of non-FSI empirical loads can be considered valid for this case.

Table 4 presents the results of the parametric study in terms of pass/fail, where '-' indicates no material failure was present, 'F_i' indicates that the panel failed in the inward direction and 'F_o' indicates that the panel failed in the outward direction, i.e. towards the direction of the blast.

With the exception of the most brittle case, where failure occurs in the inward direction under all four load cases, there is no other instance where all four models agree on the failure of the glazing panel. From the evidence provided earlier in this article, it can be said that the cubic negative phase represents 'correct' treatment of the negative phase, with the other load cases representing 'incorrect' treatment. Neglecting the negative phase, therefore, is shown to be under conservative for $\epsilon_f = 4\epsilon_e$ yet conservative for $\epsilon_f = 10\epsilon_e$, whereas modelling it as an extended Friedlander may falsely predict material failure for ductile systems.

6. SUMMARY AND CONCLUSIONS
Following the positive phase of a blast comes a period where the pressure falls below atmospheric pressure known as the negative phase. Whilst the positive phase of the blast is well understood, validation of the negative phase is rare in the literature, and as such it is often incorrectly treated or neglected altogether.

This paper reviews current methods in the literature for representing the negative phase, and provides experimental validation for comparison. Of the different methods for modelling the negative phase, the cubic expression of Granström [20] gives the best approximation both qualitatively and quantitatively.

Elastic single-degree-of-freedom systems are analysed under the different loading approximations to give an idea of the magnitude of the differences in displacement that will be seen when using the different load models. Finite element analyses are undertaken on elastic-plastic panels with material failure to further highlight the lack of agreement between the results given by the different loading models.

With so many parameters influencing whether the negative phase is conservative, non-

conservative or has no effect, it is both difficult and impractical to definitively say when the negative phase can be neglected or not. In fact, because of this it can be argued that the negative phase should not be neglected at any stage until the engineer is confident that its effects are understood.

The numerical cases shown in this study are for a limited number of structural arrangements under a limited number of blast events and are by no means an attempt at an exhaustive quantification of the influence of the form of the negative phase. Instead, the examples shown, for both the 'real-life' glazing panels and the equivalent elastic systems, should serve as a reminder that the negative phase is both important and often the effect of the negative phase is underestimated. The evidence provided in this paper should provide the research community with guidance on how to model the negative phase.

ACKNOWLEDGEMENTS

REFERENCES

[1]   F. G. Friedlander. The diffraction of sound pulses. I. Diffraction by a semi-infinite plane. *Proceedings of the Royal Society A: Mathematical, Physical and Engineering Sciences*, 186(1006):322–344, 1946.

[2]   H. S. Norville, N. Harvill, E. J. Conrath, S. Shariat, and S. Mallonee. Glass-related injuries in Oklahoma City bombing. *Journal of Performance of Constructed Facilities*, 13(2):50–56, 1999.

[3]   T. Krauthammer and A. Altenberg. Negative phase blast effects on glass panels. *International Journal of Impact Engineering*, 24(1):1–17, 2000.

[4]   L. R. Dharani and J. Wei. Dynamic response of laminated glass under blast loading: effect of negative phase. In *Structures under shock and impact VIII*, pages 181–190, Crete, Greece, 2004.

[5]   J. Wei and L. R. Dharani. Response of laminated architectural glazing subjected to blast loading. *International Journal of Impact Engineering*, 32(12):2032–2047, 2006.

[6]   M. Larcher, G. Solomos, F. Casadei, and N. Gebbeken. Experimental and numerical investigations of laminated glass subjected to blast loading. *International Journal of Impact Engineering*, 39(1):42 – 50, 2012.

[7]   M. Teich and N. Gebbeken. The influence of the underpressure phase on the dynamic response of structures subjected to blast loads. *International Journal of Protective Structures*, 1(2):219–234, 2010.

[8]   M. Teich and N. Gebbeken. Structures subjected to low-level blast loads: Analysis of aerodynamic damping and fluid-structure interaction . *Journal of Structural Engineering*, 138(5):625 – 635, 2012.

[9]   M. Yang and S. Ahmari. Investigation of effect of negative phase of blast loading on cable net curtain walls through the linearized stiffness matrix method. *International Journal of Impact Engineering*, 61(0):36 – 47, 2013.

[10]   L. M. Bryant, J. M. Erekson, and K. W. Herle. Are you positive about negative phase? In *American Society of Civil Engineers (ASCE) Structures Congress 2013*, pages 103–114. Pittsburgh, PA, USA, 2013.

[11]   C. E. Needham. *Blast Waves*. Springer, Berlin, Germany, 2010.

[12]   C. N. Kingery and G. Bulmash. Airblast parameters from TNT spherical air burst and hemispherical surface burst. Technical Report ARBRL-TR-02555, U.S Army BRL, Aberdeen Proving Ground, MD, USA, 1984.

[13]   US Department of Defence. *Structures to resist the effects of accidental explosions*. US DoD, Washington DC, USA, UFC-3-340-02, 2008.

[14]   G. F. Kinney and K. J. Graham. *Explosive Shocks in Air*. Springer, NY, USA, 1985.

[15]   D. Cormie, G. Mays, and P. Smith. *Blast effects on buildings, 2nd ed.* Thomas Telford, London, UK, 2009.

[16]   D. W. Hyde. *Conventional Weapons Program (ConWep)*. U.S Army Waterways Experimental Station,

Vicksburg, MS, USA, 1991.

[17]   D. Bogosian, J. Ferritto, and Y. Shi. Measuring uncertainty and conservatism in simplified blast models. In *30th Explosives Safety Seminar*, pages 1–26. Atlanta, GA, USA, 2002.

[18]   A. Tyas, J. Warren, T. Bennett, and S. Fay. Prediction of clearing effects in far-field blast loading of finite targets. *Shock Waves*, 21(2):111–119, 2011.

[19]   A. Tyas, T. Bennett, J. Warren, S. Fay, and S. E. Rigby. Clearing of blast waves on finite-sized targets, an overlooked approach. *Applied Mechanics and Materials*, 82:669–674, 2011.

[20]   S. A. Granström. Loading characteristics of air blasts from detonating charges. Technical Report 100, Transactions of the Royal Institute of Technology, Stockholm, 1956.

[21]   W. E. Baker. *Explosions in air*. University of Texas Press, Austin, TX, USA, 1973.

[22]   C. Gantes and N. Pnevmatikos. Elastic-plastic response spectra for exponential blast loading. *International Journal of Impact Engineering*, 30(3):323–343, 2004.

[23]   G. Randers-Pehrson and K.A. Bannister. Airblast loading model for DYNA2D and DYNA3D.Technical Report ARL-TR-1310, U.S Army Research Laboratory, Aberdeen Proving Ground, MD,USA, 1997.

[24]   Naval Facilities Engineering Command. *Blast Resistant Structures*. Alexandria, VA, DM 2.08, 1986.

[25]   US Army Corps of Engineers. *Methodology manual for the Single-Degree-of-Freedom Blast Effects Design Spreadsheets (SBEDS)*. ACE Protective Design Center, Omaha, NE, USA, PDC-TR-06-01, 2005.

[26]   N. Kambouchev, L. Noels, and R. Radovitzky. Nonlinear compressibility effects in fluid-structure interaction and their implications on the air-blast loading of structures. *Journal of Applied Physics*, 100(063519), 2006.

[27]   N. Kambouchev, L. Noels, and R. Radovitzky. Numerical simulation of the fluid-structure interaction between air blast waves and free-standing plates. *Computers & Structures*, 85(11 - 14):923 – 931, 2007.

[28]   H. L. Brode. Numerical solutions of spherical blast waves. *Journal of Applied physics*, 26(6):766–775, 1955.

[29]   J. M. Biggs. *Introduction to Structural Dynamics*. McGraw-Hill, New York, NY, USA, 1964.

[30]   C. M. Morison. Dynamic response of walls and slabs by single-degree-of-freedom analysis – a critical review and revision. *International Journal of Impact Engineering*, 32(8):1214 – 1247, 2006.

[31]   Q. M. Li and H. Meng. Pulse loading shape effects on pressure-impulse diagram of an elastic-plastic, single-degree-of-freedom structural model. *International Journal of Mechanical Sciences*, 44(9):1985 – 1998, 2002.

[32]   X. Huang, L. He, and G.W. Ma. Soil-structure interaction and pulse shape effect on structural element damage to blast load. *Journal of Performance of Constructed Facilities*, 25:400 – 410, 2011.

[33]   J. O. Hallquist. *LS-DYNA Theory Manual*. Livermore Software Technology Corporation, CA, USA, 2006.

[34]   K. V. Subramaniam, W. Nian, and Y. Andreopoulos. Blast response simulation of an elastic structure: Evaluation of the fluid-structure interaction effect. *International Journal of Impact Engineering*, 36(7):965 – 974, 2009.